Vol. 4, No. 5

Developmental Variation in Rab11-Dependent Trafficking in *Trypanosoma brucei*

Belinda S. Hall, Emma Smith, Wolfram Langer, Louisa A. Jacobs, David Goulding, and Mark C. Field*

Department of Biological Sciences, Imperial College, Exhibition Road, London SW7 2AY, United Kingdom

In *Trypanosoma brucei*, endocytosis is developmentally regulated and is substantially more active in the mammalian infective stage, where it likely plays a role in immune evasion. The small GTPase TbRAB11 is highly expressed in the mammalian stage and mediates recycling of glycosylphosphatidylinositol-anchored proteins, including the variant surface glycoprotein (VSG) and the transferrin receptor, plus trafficking of internalized anti-VSG antibody and transferrin. No function has been assigned to TbRAB11 in the procyclic (insect) stage trypanosome. The importance of TbRAB11 to both bloodstream and procyclic form viability was assessed by RNA interference (RNAi). Suppression of TbRAB11 in the bloodstream form was rapidly lethal and led to cells with round morphology and an enlarged flagellar pocket. TbRAB11 RNAi was also lethal in procyclic forms, which also became rounded, but progression to cell death was significantly slower and the flagellar pocket remained normal. In bloodstream forms, silencing of TbRAB11 had no effect on exocytosis of newly synthesized VSG, fluid-phase endocytosis, or transferrin uptake, but export of internalized transferrin was inhibited. Lectin endocytosis assays revealed a block to postendosomal transport mediated by suppressing TbRAB11. By contrast, in procyclic forms, depletion of TbRAB11 blocks both fluid-phase endocytosis and internalization of surface proteins. In normal bloodstream forms, most VSG is recycled, but in procyclics, internalized surface proteins accumulated in the lysosome. These data demonstrate that TbRAB11 controls recycling and is essential in both life stages of *T. brucei* but that its primary role is subject to developmental variation.

Endocytosis and recycling of plasma membrane components are regulated by small GTPases of the Rab family (42). Mammalian Rab11 is predominantly located in the perinuclear recycling compartment and controls recycling of a range of receptors (9, 16, 19, 26, 27, 36, 37). Recycling of plasma membrane glycosphingolipids is also dependent on Rab11 (35). The *Saccharomyces cerevisiae* homologue of mammalian Rab11, Ypt3p, is essential for growth and regulates multiple stages in the exocytic pathway (5). There is also evidence for a role for Rab11 in secretory exocytosis in mammalian cells (4). In addition, Rab11 is implicated in transcytosis in polarized epithelia, in endosome-to-*trans*-Golgi network trafficking, and in actin remodeling during cellularization in *Drosophila melanogaster* embryogenesis (34, 39, 40). The ability of Rab11 to control such diverse cellular processes depends on the specific interactions of the active GTPase with a number of different binding proteins that allow association with distinct vesicular populations and domains. Several such proteins have been identified, including the Rab-11FIP family, RAB11B/Rabphilin-11, myosin VB, PI4Kβ, and Sec15p, each of which appears to be associated with distinct aspects of Rab11 function (6, 13, 22, 24, 38, 43).

Trypanosoma brucei, the protozoan parasite responsible for human African sleeping sickness, exists in biochemically and morphologically distinct forms in the mammalian and insect vector hosts. In both life stages, vesicle trafficking to and from the surface is limited to the flagellar pocket, a specialized invagination at the base of the flagellum (29). However, rates of endocytosis in the bloodstream form (BSF) and procyclic form (PCF) are vastly different. For example, endocytic recycling of the variant surface glycoprotein (VSG) in BSF is very rapid, and the entire flagellar pocket is internalized within ~2 min (8). In contrast, uptake in procyclic cells is unusually slow, with little turnover of surface proteins (23). Differentiation between BSF and PCF stages is accompanied by changes to the expression levels of a number of proteins regulating endocytosis and recycling, including clathrin and the *T. brucei* orthologue of mammalian Rab11, TbRAB11 (17, 28).

Recent work to elucidate the finer molecular details of the BSF endomembrane system has demonstrated that TbRAB11 is an important factor (12). Receptor-mediated endocytosis, internalization of surface VSG, and fluid-phase uptake are all clathrin mediated (1, 12). The absence of both an AP-2 adaptin complex and cargo sorting is apparent at the point of entry, but after fusion with TbRAB5A-positive early endosomes, VSG is negatively selected in a second clathrin-dependent step and is rapidly returned to the plasma membrane via TbRAB11-positive structures (12). A proportion of VSG is trafficked to the late endosome, but this is also recycled to the surface by TbRAB11 (8). Like VSG, internalized anti-VSG immunoglobulins and transferrin are transported to a TbRAB5A compartment and thereafter degraded and recycled in a TbRAB11-dependent manner (32, 33). TbRAB4 does not ap-

pear to play a major part in recycling but controls the flow of fluid-phase cargo, which is segregated from endocytosed VSG and trafficked to the lysosome (14).

The endocytic system of the PCF stage is less well characterized. The PCF has a distinct surface coat that is composed of further glycosylphosphatidylinositol (GPI)-anchored proteins, called procyclins, but lacks VSG. As in BSFs, endocytosis is clathrin dependent, and internalized cargo first enters a TbRAB5A compartment, but the endosomal compartments in the PCF are less complex than in the BSF. TbRAB5A and the related TbRAB5B, which occupy distinct domains in BSF, colocalize in the PCF (32), and the clathrin-coated vesicles responsible for sorting of VSG from other cargo have not been described for PCF. Recycling of surface proteins has been reported (23), but the role of TbRAB11, which is down-regulated in this stage, is unknown (17). Here we show that TbRAB11 is essential to both major trypanosome life stages and also appears to have distinct roles.

MATERIALS AND METHODS

Cell culture. The BSF line *T. brucei* BSF90-13 Lister 427 was maintained in HMI-9 medium supplemented with 10% tetracycline-free fetal bovine serum (Autogen Bioclear) in the continuous presence of 5 μg ml^{-1} hygromycin B (Sigma) and 2.5 μg ml^{-1} Geneticin (Sigma) to maintain the T7-responsive phenotype (41). Tetracycline-responsive PTT cells, derived from strain 427 procyclic cells (a kind gift from Phillipe Bastin), were maintained in SDM-79 medium supplemented with 10% tetracycline-free fetal bovine serum and 7.5 μg ml^{-1} hemin in the presence of 25 μg ml^{-1} each of hygromycin B and Geneticin. For growth curves, triplicate cultures were initiated at 5 $\times$ 10^4 cells ml^{-1} for BSF and 1 $\times$ 10^5 cells ml^{-1} for PCF. Cell concentration was determined using a Z2 Coulter counter (Beckman Coulter).

Recombinant DNA constructs and transfections. To express double-stranded TbRAB11 RNA, the entire TbRAB11 open reading frame was excised from pSX519.TbRAB11^{WT} (33) using BamHI and HindIII and inserted into p2T7Ti (21). For BSF RNA interference (RNAi), the p2T7Ti-TbRAB11 construct was linearized with EcoRV and introduced into the tetracycline-responsive line, BSF 90-13, by electroporation, and cells were incubated for 6 h before the addition of 2.5 μg ml^{-1} phleomycin (Sigma). Selected lines were maintained thereafter in the presence of phleomycin. For procyclics, p2T7Ti-TbRAB11 was transfected into the PTT procyclic line. After 16 h of recovery, cells were selected with 2.5 μg ml^{-1} phleomycin for 4 weeks.

Western blotting. Cells were induced for various times, washed once in phosphate-buffered saline (PBS), and resuspended in sodium dodecyl sulfate (SDS) sample buffer. Cells were loaded on SDS–12% polyacrylamide gel electrophoresis (SDS–12% PAGE) gels at 10^7 cell equivalents per lane. After separation, proteins were transferred onto Hybond nitrocellulose paper (Amersham Biosciences). Membranes were blocked with PBS–5% milk–0.1% Tween 20 for 1 h at room temperature and then incubated overnight at 4°C in the presence of affinity-purified rabbit anti-TbRAB11 antibodies at a concentration of approximately 1 μg ml^{-1} in blocking buffer (17). Membranes were washed in PBS–0.1% Tween 20 and then incubated with peroxidase-conjugated goat anti-rabbit or anti-mouse immunoglobulin G (Sigma) for 1 h. Peroxidase was visualized with luminol. To ensure equality of loading, blots were stripped and reprobed with antibody to the major endoplasmic reticulum protein *T. brucei* binding protein (TbBiP) (2).

Electron microscopy. For transmission electron microscopy, cells were fixed in suspension by adding chilled 5% glutaraldehyde (TAAB) and 8% paraformaldehyde (Sigma) in PBS in a 1:1 ratio to the growth medium containing trypanosomes. Cells were fixed on ice for 10 min and centrifuged at 10,000 rpm for 5 min in 2-ml microcentrifuge tubes, and the supernatant was carefully replaced with fresh fixative for a further 50 min without disturbing the pellet, rinsed in 0.1 M sodium cacodylate, and postfixed in 1% osmium tetroxide (TAAB) in the same buffer at room temperature for 1 h. After rinsing in buffer, cells were then dehydrated in an ethanol series, with the addition of 1% uranyl acetate at the 30% stage followed by propylene oxide, then embedded in Epon/Araldite 502 (TAAB), and finally polymerized at 60°C for 48 h. Sections were cut on a Leica Ultracut-T ultramicrotome at 70 nm using a diamond knife, contrasted with uranyl acetate and lead citrate, and examined on a Philips CM100 transmission electron microscope.

Endocytosis of ConA. Cells were incubated for 14 to 18 h with 1 μg ml^{-1} tetracycline, harvested, and washed once in serum-free HMI-9 medium containing 1% bovine serum albumin (BSA) (SF/HMI-9). Cells were resuspended in SF/HMI-9 at a concentration of 10^7 ml^{-1} and incubated at 4 or 37°C for 20 min. Fluorescein isothiocyanate-concanavalin A (FITC-ConA; 10 μg ml^{-1}) was added, and the cells were incubated for a further 30 min. Uptake was stopped by placing cells on ice. Labeled cells were washed in SF/HMI-9 at 4°C, then fixed by incubation for 1 h at 4°C in 4% paraformaldehyde, and then adhered to slides. Cells were permeabilized with 0.1% Triton X-100 for 5 min and blocked with 10% goat serum in PBS. Slides were counterstained with affinity-purified polyclonal rabbit antibody against clathrin heavy chain (28) or the anti-p67 monoclonal antibody MAb280 (18) followed by Texas Red-conjugated goat anti-rabbit or anti-mouse antibodies (Molecular Probes) as appropriate. Cells were examined under a Nikon Eclipse E600 microscope, and images were captured using a Photometrix Coolsnap FX camera controlled with Metamorph (Universal Imaging Corp.) and assembled in Photoshop (Adobe Inc).

Fluid-phase endocytosis. Cells were induced with tetracycline as required and resuspended at a concentration of 5 $\times$ 10^8 ml^{-1} in 50-μl aliquots of fresh complete medium. Alexa Fluor 488-labeled dextran 10,000 (Molecular Probes) was added to a concentration of 5 mg ml^{-1}. Cells were incubated for various times, and accumulation was stopped by the addition of 1 ml cold medium. Cells were washed and fixed in 4% paraformaldehyde for 1 h before being mounted onto poly-L-lysine slides (Sigma). Images were captured by using identical exposure times under nonsaturating conditions. Fluorescence was quantified using Metamorph.

Uptake of biotinylated surface proteins in procyclic cells. Uptake of biotinylated proteins was followed by a modification of the method described previously (8). Uninduced PTT p2T7Ti-TbRAB11 cells were harvested in mid-logarithmic phase, washed twice in ice-cold PBS, pH 7.4, containing 1 mg ml^{-1} glucose, then resuspended in 1 ml of PBS-glucose, and incubated for 10 min on ice with 1 mg ml^{-1} Sulfo-NHS-SS-biotin (Pierce). Labeling was stopped by the addition of 100 μl of 1 M Tris-HCl, pH 7.4. Cells were washed once in cold SDM-79 medium, resuspended at a concentration of 10^8 cells ml^{-1} in SDM-79, and incubated for various times at 28°C. Cells were washed once in ice-cold SDM-79, and surface biotin was stripped by incubation for 15 min at 4°C in 50 mM reduced glutathione (Sigma) in SDM-79, pH 8.5, before fixation. Biotin was detected with Texas Red-conjugated streptavidin (Vectalabs). For quantification, images were taken under identical, nonsaturating conditions.

Transferrin endocytosis and recycling. Bovine *holo*-transferrin (Sigma) was iodinated with iodine-125 (Amersham Biosciences) by using IodoBeads reagent (Pierce) following the manufacturer's instructions. Assays were carried out as described previously (14). Briefly, the expression of double-stranded RNA corresponding to TbRAB11 in p2T7Ti-TbRAB11 cells was induced for 16 to 18 h with 1 μg ml^{-1} tetracycline. Cells were washed twice with SF/HMI-9. Washed cells were incubated at 37°C for 30 min at a concentration of 1 $\times$ 10^7 to 2 $\times$ 10^7 cells ml^{-1}, and then ^{125}I-labeled transferrin was added (typically ~2 μg at a specific activity of 3 $\times$ 10^6 cpm μg^{-1}). Triplicate 500-μl samples of cells were incubated at 4 or 37°C for various times. Nonspecific binding controls included cold transferrin at a concentration of 600 μg ml^{-1}. Accumulation was stopped by the addition of 500 μl of cold SF/HMI-9 containing 600 μg ml^{-1} transferrin. Cells were washed three times in ice-cold PBS–0.05% BSA and resuspended in 200 μl PBS. Accumulation of ^{125}I was measured with a γ-counter (Beckman Coulter). For the recycling of transferrin degradative products, cells were pulsed for 40 min with transferrin, washed in PBS-BSA as described above, and then resuspended to a final concentration of 2 $\times$ 10^7 cells ml^{-1} in complete HMI-9. Cells were incubated for 20 min at 37 or 4°C and then centrifuged for 1 min at 13,000 $\times$ *g* at 4°C. Radioactivity in supernatants and pellets was determined as described above.

VSG export assay. Export was monitored as described previously (1). Briefly, 5 $\times$ 10^7 mid-log-phase BSF cells were washed once in labeling (Met/Cys-free Dulbecco's minimal essential medium [Sigma] supplemented with 10% dialyzed fetal calf serum and HEPES, pH 7.4), resuspended in 1 ml labeling medium, and incubated at 37°C for 15 min. The cells were pulse-labeled at 37°C for 7 min with Promix at a concentration of 200 μCi/ml, then diluted 1:10 with prewarmed complete HMI-9, and chased for up to 1 h at 37°C. At intervals during the chase, aliquots of cells were removed from the sample and placed on ice. Following centrifugation in a microcentrifuge (20,000 $\times$ *g* at 4°C), cell pellets were washed once in 1 ml ice-cold PBS–1 mg/ml BSA and resuspended in 920 μl of hypotonic lysis buffer (1). After 5 min on ice, the lysates were incubated at 37°C for 10 min to enable GPI-specific phospholipase C to convert susceptible membrane-form VSG to soluble VSG. Lysates were centrifuged for 10 min at
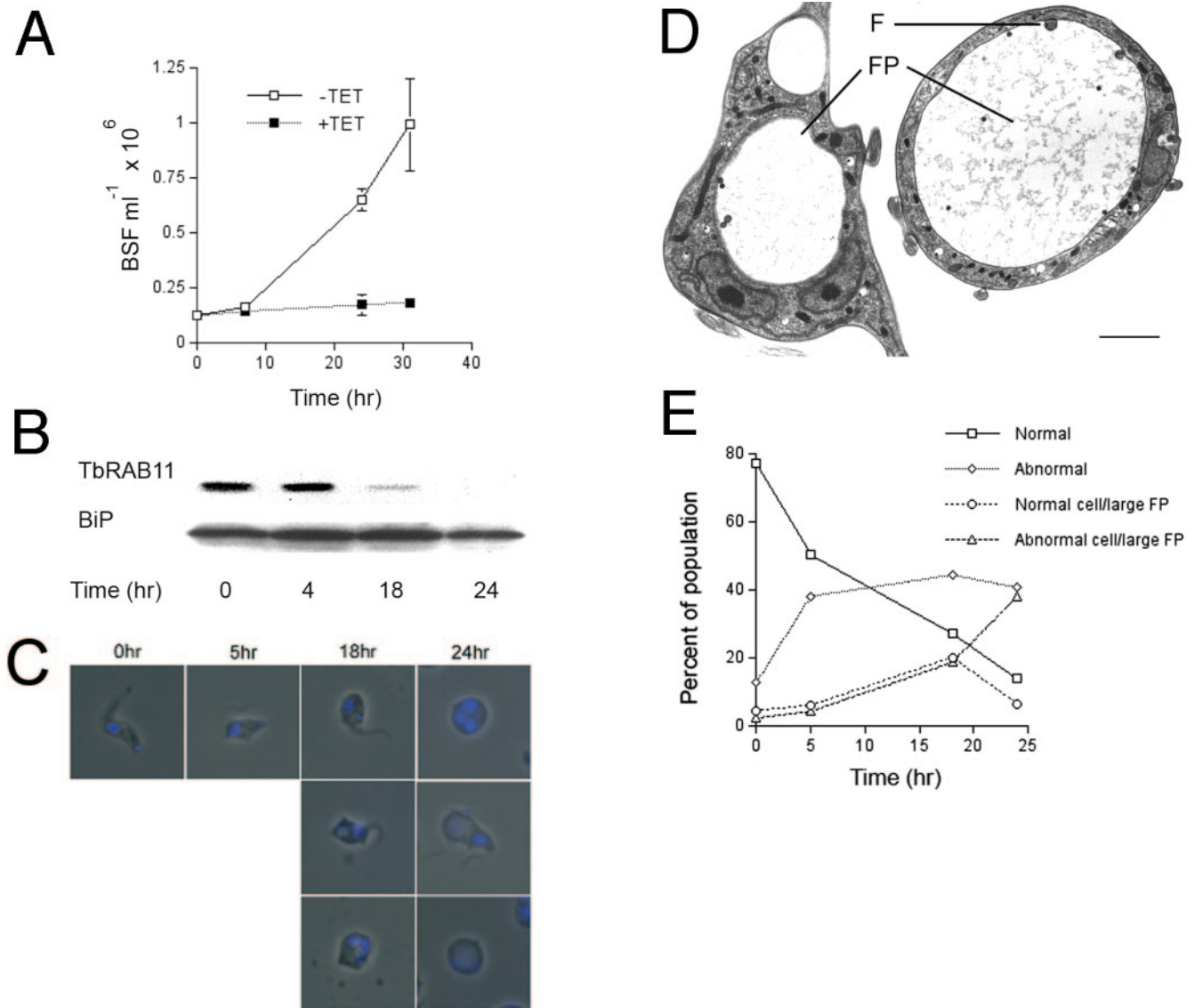
FIG. 1. TbRAB11 is essential in BSF *T. brucei*. (A) Growth of p2T7Ti-TbRAB11 BSF 20-19 cells cultured in the absence (open squares) and presence (filled squares) of 1 μg ml^{-1} tetracycline. Each data point represents the mean of triplicate counts ± the standard deviation. This result is typical of multiple repeated experiments. (B) Western blot analysis of TbRAB11 protein expression levels. p2T7Ti-TbRAB11 BSF cells were incubated in the presence of 1 μg ml^{-1} tetracycline for 0, 4, 18, and 24 h before the harvesting and separating of proteins by SDS-PAGE. Blots were probed with affinity-purified rabbit anti-TbRAB11 protein, stripped, and reprobed with rabbit anti-TbBiP antibody. Each lane contains 10^7 cell equivalents. (C) Morphology of p2T7Ti-TbRAB11 BSF cells incubated with 1 μg ml^{-1} tetracycline for various time points. Cells were harvested and fixed in 4% paraformaldehyde, washed in PBS, and adhered to poly-L-lysine slides. Nuclei and kinetoplasts are shown blue with DAPI. Note the rounding up of cells at later time points. (D) Electron micrographs of p2T7Ti-TbRAB11 BSF cells incubated in the presence of 1 μg ml^{-1} tetracycline for 24 h. F, flagellum; FP, flagellar pocket. The black bar represents 1 μm. (E) Quantitation of morphological changes in tetracycline-induced cells. At least 100 cells were counted for each time point. Abnormal is defined as any change in cell shape, from shortening of the cell body to complete rounding of the cell. Note that flagellar pocket enlargement occurs after the appearance of abnormal cells.

20,000 × g at 4°C, and 900 μl of supernatant was retained. The pellet fraction was washed in ice-cold hypotonic lysis buffer, resuspended in 1 ml ice-cold sample lysis buffer (1), and incubated on ice for 25 min. Ninety microliters of 10× sample lysis buffer and 10 μl of NP-40 were added to the supernatant fraction to bring all of the samples into the same buffer. Lysates were clarified by centrifugation for 15 min (20,000 × g, 4°C). Labeled VSG was recovered from the supernatants by incubation for 1 h at 4°C with ConA Sepharose 4B in the presence of 1 mM CaCl$_2$ and 1 mM MnCl$_2$. After being washed, samples were resuspended in sample buffer and loaded onto SDS–10% PAGE gels at 10^5 cell equivalents per lane. Fixed, stained gels were treated for 1 h with En³Hance (Perkin-Elmer) and autoradiographed. Image intensity was quantified using NIH Image.

RESULTS

TbRAB11 is essential in both bloodstream and procyclic form trypanosomes. Induction of expression of double-stranded TbRAB11 RNA leads to an immediate cessation of growth in the BSF, paralleled by a loss of expression of the TbRAB11 protein (Fig. 1A and B). By phase-contrast microscopy, abnormally shortened cells began to appear within a few hours of induction. Cells became progressively more rounded with time, and an enlarged vacuole became visible after ~18 h

(Fig. 1C). To identify the large vacuole, the ultrastructure of TbRAB11 RNAi cells was analyzed by electron microscopy (Fig. 1D). The presence of a flagellum clearly identifies the swollen structure that takes up most of the cell body as the flagellar pocket. Although the morphological phenotype triggered by TbRAB11 loss is superficially similar to the BigEye phenotype characteristically induced by a block in endocytosis (1, 15), the kinetics are distinct. RNAi of clathrin leads to an increase in the size of the flagellar pocket as the first morphologically detectable feature (1), but for TbRAB11 suppression, cell rounding precedes flagellar pocket enlargement and only a small proportion of cells retain normal cell shape (Fig. 1E). Hence, in this case, flagellar pocket enlargement is probably a secondary effect, presumably due to overall imbalance in trafficking at the plasma membrane. Analysis of DAPI (4′,6′-diamidino-2-phenylindole)-stained cells revealed similar kinetoplast-to-nucleus ratios and copy numbers in both induced and uninduced cells, suggesting that growth arrest was not associated with a specific block in the cell cycle (data not shown).

In the PCF, TbRAB11 is expressed at much lower levels than in the BSF (17), and the effects of TbRAB11 depletion in this life stage were both less immediate and less dramatic than for BSFs. Partial growth inhibition was detectable 2 days postinduction, but complete inhibition of cell division was obtained only after 3 days of induction (Fig. 2A). A marked decrease in TbRAB11 protein was detected after only 28 h and prior to a significant growth defect (Fig. 2B), suggesting that the PCF is tolerant of reduced TbRAB11 levels. However, similar to the BSF cells, PCF cells become gradually more round (Fig. 2C). At 4 days, approximately 75% of cells retain normal morphology despite complete inhibition of growth. By electron microscopy, the intracellular morphology of the PCFs 3 days after the addition of tetracycline is apparently normal, even in rounded cells, with no increase in the size of the flagellar pocket (Fig. 2D). Thus, as well as a slower response to the loss of TbRAB11, PCF cells exhibit much less severe ultrastructural defects than BSF cells. However, the inhibition of growth in both BSF and PCF cells demonstrates that TbRAB11 expression is essential for both of the major proliferative life stages of *T. brucei*.

TbRAB11 is necessary for recycling transferrin and delivery of endocytosed cargo to the lysosome in the BSF but is not required for early stages of endocytosis. TbRAB11 compartments are associated with internalized surface proteins, and biotinylated VSG recycling from the early and late endosomes is consistently found in TbRAB11-positive vesicles (12, 17). Indirect analyses of turnover of fluorescent transferrin and anti-VSG antibodies also suggest that TbRAB11 is involved in recycling (33), but no direct measurements have been made to date. To confirm the role of TbRAB11 in the endocytic pathway, bulk uptake and recycling of radiolabeled transferrin were assayed in BSF TbRAB11 RNAi cells. TbRAB11 expression was not required for endocytosis of transferrin, but recycling of the internalized protein was reduced by approximately 80% (Fig. 3A).

This was unexpected, since inhibition of transferrin receptor recycling should lead to a gradual inhibition of uptake, and recent reports have suggested that inhibition of TbRAB11 leads to a relocalization of the transferrin receptor from the
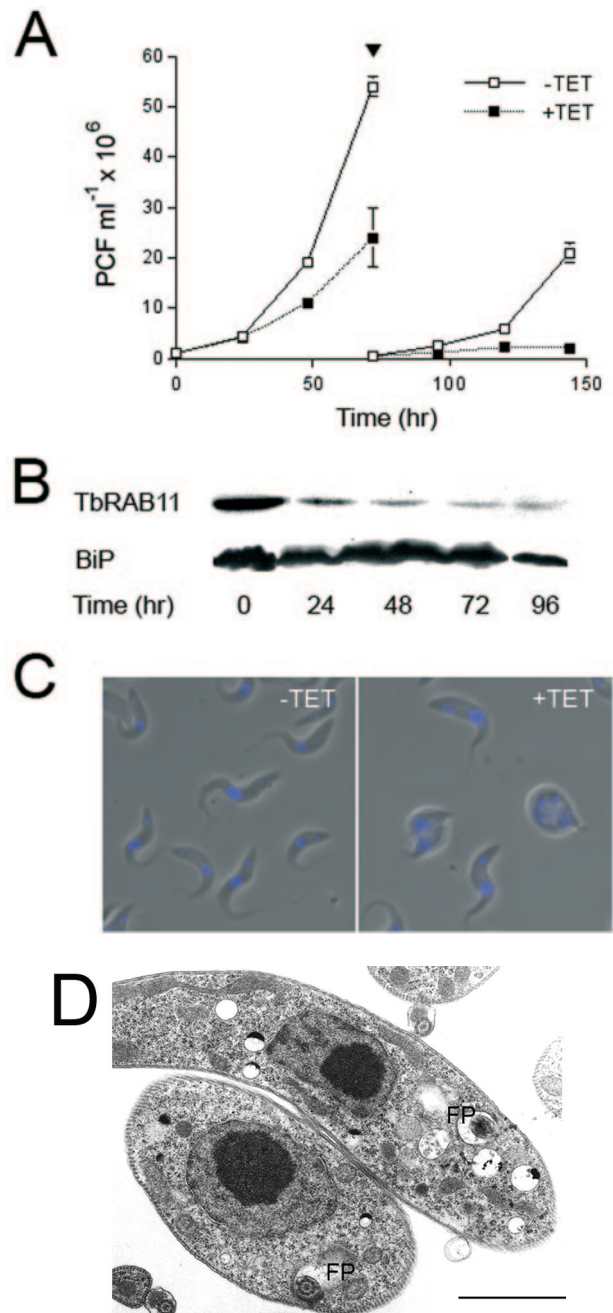

FIG. 2. TbRAB11 is essential in PCF *T. brucei*. (A) Growth rates of p2T7Ti-TbRAB11 PTT cells cultured in the absence (open squares) and presence (filled squares) of 1 μg ml^{-1} tetracycline. Each point represents the mean of triplicate counts ± the standard deviation. The arrowhead indicates dilution of culture. This result is typical of multiple repeated experiments. (B) Western blot analysis of TbRAB11 expression levels. p2T7Ti-TbRAB11 PCF cells were incubated in the presence of 1 μg ml^{-1} tetracycline for various times. Blots were probed with affinity-purified rabbit anti-TbRAB11 protein and then stripped and reprobed with rabbit anti-TbBiP antibody. Each lane contains 10^7 cell equivalents. (C) Phase-contrast morphology of cells incubated for 4 days in the presence or absence of tetracycline. Cells are stained with DAPI to visualize the nucleus and kinetoplast (blue). (D) Electron micrograph of p2T7Ti-TbRAB11 PTT PCF incubated with tetracycline for 3 days. The black bar represents 1 μm. FP, flagellar pocket.
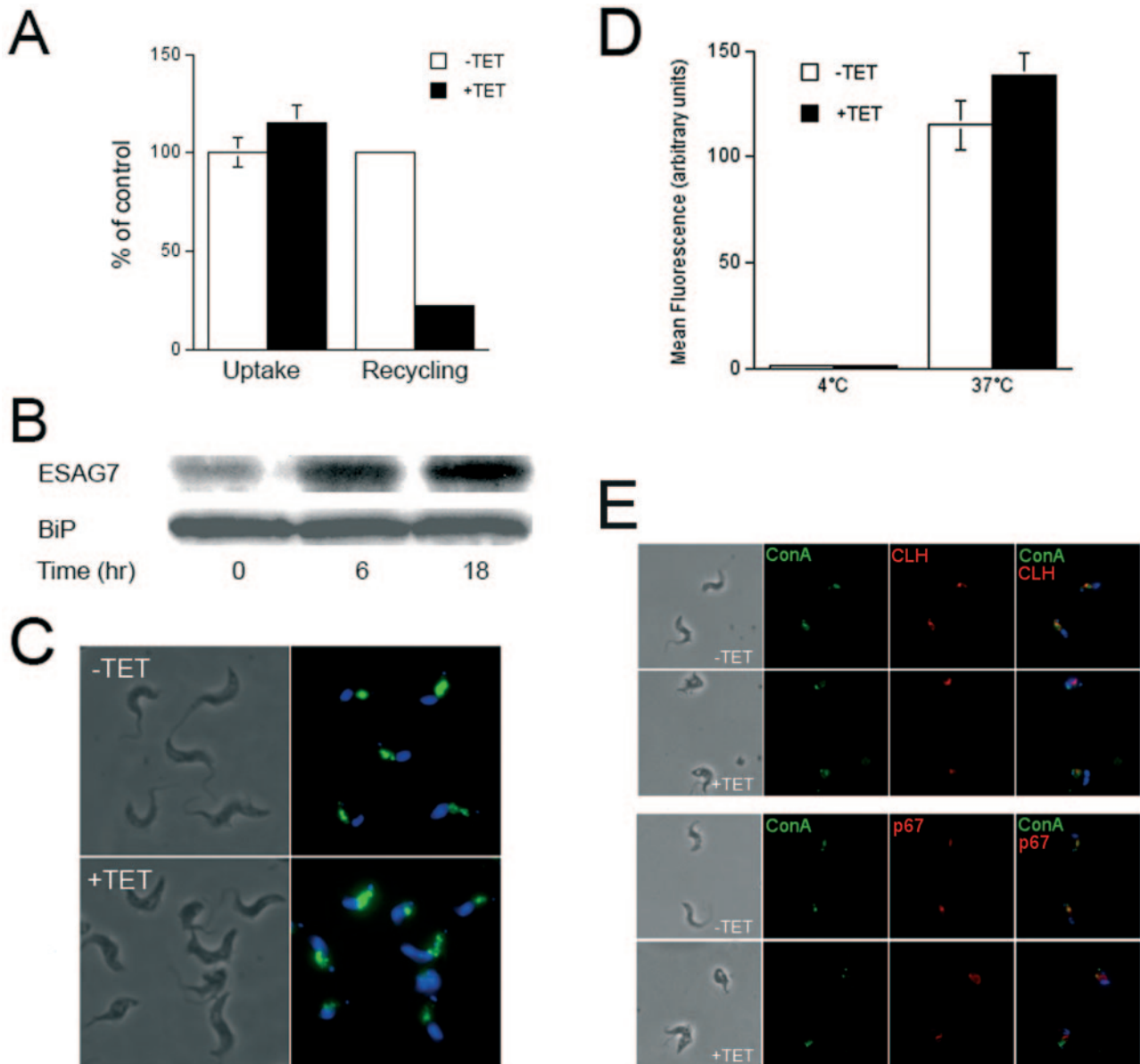
FIG. 3. TbRAB11 RNAi blocks transferrin recycling and endocytic trafficking of ConA. (A) Uptake and recycling of ^{125}I-labeled bovine transferrin by p2T7Ti-TbRAB11 BSF cultured in the absence (open bars) and presence (filled bars) of 1 μg ml^{-1} tetracycline for 18 h. Cells were incubated at 37°C with label for 40 min. Results are presented as the percentages of radioactivity above background in untreated cells. For recycling, labeled cells were washed and reincubated at 37°C. Recycling was calculated as the percentage of total label in the supernatant compared to a background of cells incubated at 4°C. For uptake, results are presented as a percentage of recycling in untreated cells. All results are the means of triplicate measurements $\pm$ the standard errors of the means (SEM). These data are representative of multiple repeated experiments. (B) p2T7Ti-TbRAB11 BSF cells were induced with 1 μg ml^{-1} tetracycline for various times before harvesting. Blots of whole-cell lysates (5 $\times$ 10^6 cell equivalents per lane) were probed with rabbit anti-transferrin receptor antibody recognizing the ESAG7 subunit. (C) Fluid-phase uptake in TbRAB11 RNAi of bloodstream form cells. p2T7Ti-TbRAB11 BSF cells were induced for 14 h with (+TET) or without (−TET) tetracycline and then incubated for 30 min with Alexa Fluor 488 dextran 10,000 (green). Fixed cells were counterstained with DAPI (blue) and examined immediately. (D) Quantitation of fluid-phase uptake. Accumulation of fluorophore in uninduced (open bars) and induced (filled bars) p2T7Ti-TbRAB11 BSF labeled at 4 or 37°C as described above was measured for images captured under identical, nonsaturating conditions using Metamorph imaging software. Values represent the mean fluorescences for at least 60 cells $\pm$ SEM. The results shown are typical of duplicate experiments. (E) Uptake of FITC-labeled ConA (green) into cells incubated in the presence or absence of 1 μg ml^{-1} tetracycline for 18 h. Cells were labeled with 10 μg ml^{-1} FITC-ConA for 30 min at 37°C. Fixed and permeabilized cells are counterstained with anticlathrin antibody (red; upper panels) or anti-p67 antibody (red; lower panels). Nuclei and kinetoplasts are stained with DAPI (blue). Note colocalization of internalized ConA with the lysosomal marker p67 in untreated cells. Quantitation shows 50% $\pm$ 4.6% of ConA colocalizes with p67 in induced cells, compared with 86% $\pm$ 2.3% in uninduced cells (n = 30). Results are typical of multiple experiments.

flagellar pocket to intracellular sites (31). However, the *T. brucei* BSF can compensate for a reduction in iron availability with increased expression of the transferrin receptor ESAG6/7 (10). To investigate whether TbRAB11 RNAi induction alters transferrin receptor expression, whole-cell lysates were prepared at different times of exposure to tetracycline. By Western blotting, the total level of the ESAG7 subunit of the receptor increased with time in induced cells (Fig. 3B). A similar increase was observed in ESAG6 expression (data not shown). No change was seen in TbBiP or in total VSG levels (data not shown), indicating that the increase in ESAG6/7 expression was specific. Thus, a balance between synthesis and degradation of the receptor may allow transferrin uptake to be maintained at a constant level even in a background where endocytic flux is reduced, consistent with previous data that show that these proteins are tightly regulated by iron availability. It is unclear what happens to the internalized transferrin, but it is possible that cargo and receptor accumulate in similar internal sites. Overall, these data indicate a decrease in the flux of receptor-mediated endocytosis in TbRAB11-suppressed cells.

The pathway for transport of fluid-phase cargo in the *T. brucei* BSF is distinct from that taken by GPI-anchored proteins. Fluorescent dextran separates from surface proteins very rapidly following entry into the cell. While most VSG is recycled directly or via the late endosome (8), fluid-phase traffic is accumulated in the lysosome in a process regulated by TbRAB4 (14). Based on current understanding, changes to TbRAB11 expression would therefore be predicted to have little impact on fluid-phase transport in the BSF, and this is indeed the case (Fig. 3C and D). Although a reduction in uptake of Alexa Fluor 488-labeled dextran can be seen in the most severely deformed cells (Fig. 3C, arrows), most parasites accumulate dextran normally when TbRAB11 is depleted and no significant change in mean fluorescence is detectable (Fig. 3D).

To analyze the fate of endocytosed cargo, trafficking of internalized material was monitored by allowing cells to take up FITC-labeled ConA and then costaining for clathrin or the lysosomal marker p67 (Fig. 3E). On entry into the cell, ConA is initially transported via clathrin-coated vesicles to the TbRAB5A-positive early endosome and thence to the lysosome (1, 3, 17). In both uninduced and induced TbRAB11 RNAi cells, there is little overlap between FITC-ConA and clathrin after 30 min, indicating that trafficking to the early endosome does not require TbRAB11. However, transport to the lysosome is affected by TbRAB11 suppression. While the majority of ConA is located within the p67 compartment in uninduced cells, FITC-ConA and anti-p67 labeling are distinct in induced cells. Quantitation of the degree of colocalization confirmed a significant decrease in ConA trafficking to the lysosome ($P < 0.001$).

TbRAB11 is not required for exocytosis of newly synthesized VSG. Both Ypt3p, the yeast orthologue of TbRAB11, and mammalian Rab11 function in the exocytic pathway (4, 5). Immunoelectron microscopy has failed to identify TbRAB11-negative exocytic vesicles carrying VSG, raising the possibility that TbRAB11 mediates the export of both newly synthesized and recycled VSG (31). However, as biosynthetic VSG represents only a small proportion of total intracellular VSG, exocytic VSG vesicles may have been overlooked by morphologi-
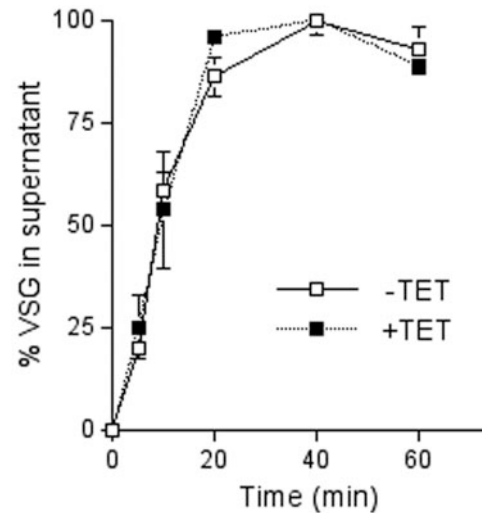

FIG. 4. TbRAB11 is not required for export of newly synthesized VSG. Export of VSG in uninduced (open squares) and 18 h induced (filled squares) p2T7Ti-TbRAB11 BSF cells was monitored by recovery of GPI-specific phospholipase C-hydrolyzed soluble VSG from supernatants of hypotonic lysates taken at different time points following pulse labeling with [^{35}S]methionine (1). Soluble VSG was quantified by densitometric analysis of labeled bands on autoradiograms using NIH Image software. Results are presented as percentages of total recovered VSG in the supernatant after background subtraction. Each time point shows the mean of duplicate experiments ± the range.

cal analysis. To determine whether TbRAB11 has a role in the exocytosis of newly synthesized proteins, the rate of transport of ^{35}S-labeled VSG from the endoplasmic reticulum to the cell surface was monitored (1, 7). In uninduced cells, VSG reaches the surface with a half time of approximately 9 min. Neither the rate of transport nor the proportion of VSG recovered in the supernatant was altered by suppression of TbRAB11 (Fig. 4). By contrast, suppressing either TbRAB1 or TbRAB2, proteins regulating endoplasmic reticulum-to-Golgi and intra-Golgi transport, leads to a significant decrease in the rate of VSG exocytosis (7). These data therefore indicate that TbRAB11 is unlikely to be a key component of the biosynthetic VSG exocytic pathway.

TbRAB11 RNAi blocks endocytosis in procyclics. The role of TbRAB11 in PCF endocytic trafficking was assessed by monitoring uptake of fluorescent dextran. In contrast to the lack of effect on fluid-phase transport in the BSF, transport of dextran was inhibited in procyclics by TbRAB11 suppression (Fig. 5A and B). This suggests that control of fluid-phase trafficking is different for the two life stages and that TbRAB11 may have distinct roles in PCF and BSF cells. To determine whether the loss of TbRAB11 also affected the internalization of plasma membrane proteins, the cell surface was labeled with cleavable biotin and cells were incubated for various times. Remaining external label was stripped with glutathione and internal biotin detected with Texas Red-labeled streptavidin. Unstripped cells showed staining of the entire surface, with the strongest signal on the flagellum and in the flagellar pocket, a pattern similar to that obtained by staining with FITC-labeled ConA, and no difference in intensity could be detected between TbRAB11 RNAi and control cells (data not shown). A low level of biotin
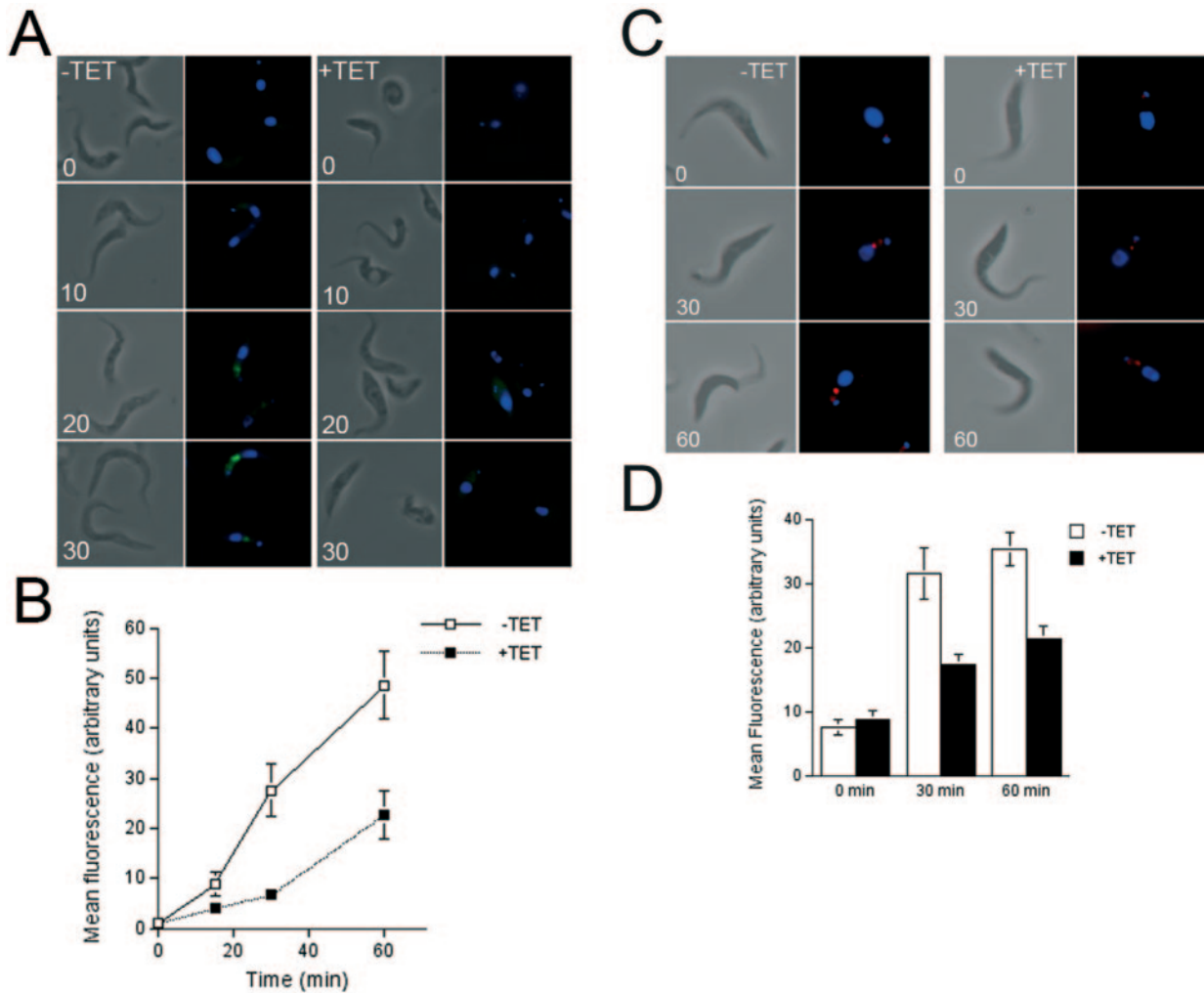
FIG. 5. Endocytosis is inhibited by TbRAB11 RNAi in procyclic cells. (A) Fluid-phase uptake is blocked in PCF cells lacking TbRAB11. p2T7Ti-TbRAB11 PTT cells were induced for three days with (+TET) or without (−TET) tetracycline and then incubated at 28°C with Alexa Fluor 488 dextran 10 000 (green) for various times. Cells were fixed as described in the text, counterstained with DAPI (blue), and examined immediately. (B) Quantitation of fluid-phase uptake. Accumulation of fluorophore in uninduced (open squares) and induced (filled squares) p2T7Ti-TbRAB11 PTT cells labeled as described above was measured using Metamorph Imaging software. Data represent the signal above background for at least 50 cells ± SEM. The results shown are typical of duplicate experiments. (C) Inhibition of internalization of biotinylated surface proteins in the PCF under TbRAB11 RNAi. p2T7Ti-TbRAB11 PTT cells were induced for 3 days with (+TET) or without (−TET) tetracycline and then labeled with biotin. Cells were allowed to internalize surface proteins at 28°C for various times, and then external biotin was stripped. Internal biotin was visualized with Texas Red streptavidin, and slides were counterstained with DAPI (blue). (D) Quantitation of biotin internalization. Accumulation of biotin in uninduced (open bars) and induced (filled bars) p2T7Ti-TbRAB11 PTT cells labeled for various times as described above was measured using Metamorph Imaging software. Data represent the signal above background for at least 30 cells ± SEM.

was seen in cells incubated at 4°C that appeared to be restricted to the flagellar pocket (Fig. 5C). In cells incubated at 28°C for 30 min, internalized biotin was detected in endosomal compartments. Intracellular biotin levels increased over time in both induced and uninduced cells, but, as seen for fluid-phase trafficking, levels of fluorescence were consistently reduced in cells lacking TbRAB11 expression (Fig. 5C and D). Thus, TbRAB11 loss leads to a reduction in both fluid-phase and membrane protein endocytic activity in the PCF.

Internalized surface protein and fluid-phase cargo both accumulate in the lysosome in PCF parasites. As in the BSF, the surface coat of the PCF is predominantly made up of GPI-anchored proteins, so the distinct patterns of fluid-phase and

membrane protein transport in PCF and BSF TbRAB11 RNAi cannot be attributed to differential trafficking of GPI- versus non-GPI-anchored proteins. In the BSF, biotinylated VSG and fluid-phase cargo become rapidly separated, and at steady state only approximately 20% of endocytosed VSG colocalizes with dextran (8). TbRAB11 RNAi has similar effects on both fluid-phase uptake and internalization of surface protein in the PCF, suggesting that these cells may not segregate cargo to the same degree as BSFs. To investigate the relationships between fluid-phase and surface protein trafficking pathways, procyclic cells were labeled with both biotin and Alexa 488 dextran. After 1 h, internalized biotin and dextran were almost completely colocalized (Fig. 6A). Quantitation indicates colocalization of
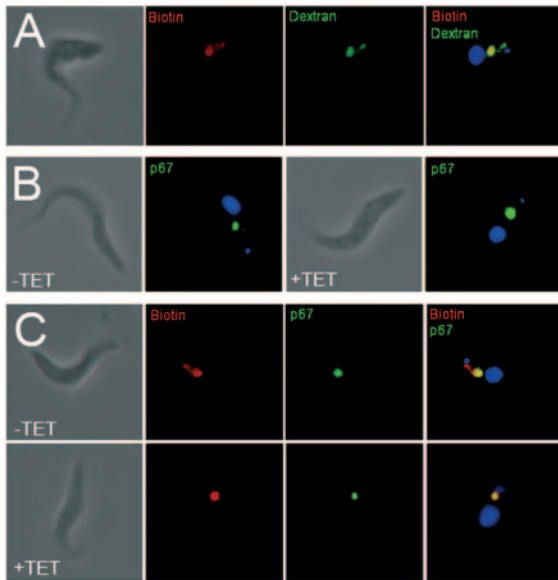
FIG. 6. Fluid-phase marker and internalized surface protein both accumulate in the lysosome in the *T. brucei* PCF. (A) Fluid-phase markers colocalize with internalized surface protein in uninduced PCF cells. Uninduced p2T7Ti-TbRAB11 PCF cells were surface labeled with biotin and allowed to take up Alexa Fluor 488 dextran 10 000 (green) for 1 h at 28°C. External biotin was cleaved, and internalized biotin was visualized with Texas Red-labeled streptavidin (red). Slides were counterstained with DAPI (blue) and examined immediately. (B) Loss of TbRAB11 causes enhanced p67 staining in PCF. p2T7Ti-TbRAB11 PTT cells were incubated for 3 days with (+TET) or without (−TET) tetracycline. Cells were fixed, permeabilized, and stained with MAb280 against p67. Bound antibody was detected with Alexa Fluor 488-conjugated goat anti-mouse antibody (green) and counterstained with DAPI (blue). (C) Colocalization of internalized surface proteins with p67. p2T7Ti-TbRAB11 PTT cells were incubated for 3 days with (+TET) or without (−TET) tetracycline and then labeled with biotin as described for panel B. Cells were incubated for 1 h at 28°C, stripped of surface biotin, fixed, and permeabilized before staining with Texas Red streptavidin (red) and MAb280 (green). Low concentrations of MAb280 were used to increase the specificity of signal. Cells were counterstained with DAPI (blue).

80.3% ± 3.7% ($n = 33$) for the two fluorophores and suggests that, in contrast to VSG in the BSF, most PCF surface proteins and endocytosed fluid-phase cargo follow similar routes.

In the normal BSF, fluid-phase cargo is trafficked to the lysosome (8, 14). To determine whether the inhibition seen by TbRAB11 suppression was due to effects on the lysosome, induced and uninduced cells were stained with antibody to p67 (Fig. 6B). Loss of TbRAB11 expression led to an increase in intensity of staining of the PCF p67 compartment. The increased staining suggests enhanced p67 synthesis and trafficking, inhibition of trafficking at a postlysosomal step, or a general rerouting of material that would otherwise be recycled towards the lysosome. In order to distinguish between these possibilities, PCF cells were costained for internalized biotin and p67 (Fig. 6C). For the purposes of colocalization, images were captured under limiting conditions to minimize signal crossover, which explains the reduced level of p67 staining in the induced cells. In the BSF, very little internalized VSG is found in the lysosomal compartment (8), but in both uninduced and induced procyclic cells, the bulk of the internalized

biotin label colocalized with p67. The proportion of internalized label found in the lysosomal compartment was unchanged (76.1% ± 2.6% for induced cells and 79.7% ± 3.3% for uninduced cells). Taken together, the results show in PCF trypanosomes most endocytic cargo is directed to the lysosome.

DISCUSSION

Endocytosis is developmentally regulated in *T. brucei* and affects both nutrient uptake and drug sensitivity (29). In addition, VSG in BSF parasites is efficiently recycled in a process that also removes bound immune effectors, suggesting an important role in immune evasion. Studies in this laboratory and others have implicated TbRAB11 in the recycling of VSG and the transferrin receptor as well as the export of degraded anti-VSG antibody and transferrin (12, 33). Maintenance of the uptake arm of the endocytic system is essential to the survival of *T. brucei* (1, 15), but the importance of the recycling step to cell viability has not been established.

Here we have demonstrated that both mammal- and insect-infective *T. brucei* cells require TbRAB11 function for continued cellular survival, but ablation of TbRAB11 expression reveals distinct properties in the two cell types. First, loss of TbRAB11 expression in the BSF is rapidly lethal and induces a shortened and progressively rounded morphology. Prolonged induction of TbRAB11 RNAi leads to an enlarged flagellar pocket similar to that caused by inhibition of endocytosis (1). Second, TbRAB11 suppression has no effect on the kinetics of VSG delivery to the plasma membrane, which indicates that TbRAB11 is unlikely to be a significant mediator of biosynthetic VSG export. Third, in the PCF the cells also become gradually more rounded but show no change to flagellar pocket architecture. These distinct rates of response and morphological effects induced by TbRAB11 RNAi suggest that TbRAB11 may have different functions in these two life stages, as well as reflecting the markedly greater rate of endocytosis in bloodstream forms. Fourth, analysis of endocytic function following suppression of TbRAB11 reveals additional developmental differences; in the BSF, the initial stages of both receptor-mediated and fluid-phase endocytosis are unimpaired, but the recycling of degraded transferrin is almost completely blocked. By contrast, TbRAB11 suppression in the PCF leads to profound inhibition of both fluid-phase and membrane protein endocytosis. These observations indicate that the key site of TbRAB11 function in the PCF is distinct from that in the BSF, and in contrast to the multiple endocytic pathways in the BSF, the vast majority of PCF traffic appears to be directed toward the lysosome.

At least two unanticipated aspects to the trypanosome trafficking system have been uncovered in this study. Based primarily on an inability to detect secretory vesicles containing VSG but lacking associated TbRAB11, it has been proposed that TbRAB11 transport vesicles represent the sole route of export for both recycling and newly synthesized VSG (31). As almost all intracellular VSG participates in recycling and only a very small proportion of VSG is en route to the surface for the first time, the detection of putative dedicated biosynthetic transporters by morphological analysis is challenging. However, the data presented here indicate that TbRAB11 is not required for VSG export. Either TbRAB11 is present on exo-

cytic vesicles carrying newly synthesized VSG but does not have an essential role, or a second, and so far uncharacterized, pathway must be present for transport of newly synthesized VSG to the cell surface. Our second finding extends previous observations that uncovered a mechanism for cellular response to iron deprivation (30). These earlier studies were based on limiting the effective concentration of transferrin, but here we have shown that the trypanosome is capable of sensing a decrease in iron uptake due to partial inhibition of endocytic activity by an increase in the copy number of the receptor protein, compensating for a decrease in endocytic flux. Hence, a sophisticated signaling system appears to subtend the transferrin receptor to ensure adequate accumulation of iron.

Cell- or development-specific Rab11 functions have been reported for other systems. For example, mammalian Rab11b specifically regulates Ca^{2+}-dependent exocytosis in neuronal but not nonneuronal cells (20), and in *Entamoeba histolytica* Rab11 location alters during encystation, suggesting a changing role during differentiation (25). PCF trypanosomes, which have a low rate of endocytosis, do not separate surface proteins from fluid-phase cargo in the same manner as the more endocytically active BSFs. In BSFs, the Rab5 isoforms TbRAB5A and TbRAB5B have distinct functions in clathrin-mediated endocytosis, while in PCFs they occupy the same compartment and have similar effects on fluid-phase endocytosis (11, 15, 32). The expression of constitutively active TbRAB5A is also associated with an increased uptake of low-density lipoprotein, but this accompanies an increase in receptor expression (32). Altered TbRAB4 function affects fluid-phase endocytosis in BSFs but interferes with both fluid-phase and surface protein endocytosis in PCFs, again indicating a less diversified system in PCFs (14; B. S. Hall and M. C. Field, unpublished observations). Hence, the lack of differentiation between fluid-phase and receptor-mediated endocytosis, as detected in the procyclic cells, and the discrimination between these two endocytic processes in BSFs by suppression of TbRAB11 are fully consistent with previous data. In addition, as well as recycling GPI-anchored proteins from the early endosome to the surface, TbRAB11 regulates recycling from the late endosome (8) and may be required for maintenance of both directions of the pathways between early and late endosomes.

The differences in regulation of endocytosis between the two life stages may reflect the different requirements for survival in insect and mammalian hosts. The developmental regulation of TbRAB11 function in *T. brucei* may be secondary to the general changes in endocytosis between the two stages but could also be a result of differential expression of TbRAB11 binding proteins leading to preferential association with different vesicle populations within the endomembrane system. Mammalian Rab11 is capable of interacting with a variety of different proteins that target the GTPase to distinct compartments and allow participation in multiple functions (38). Identification of the TbRAB11 effectors present in the BSF and the PCF will be needed to determine the mechanism of TbRAB11 action in the different life stages.

ACKNOWLEDGMENTS

REFERENCES

1. **Allen, C. L., D. Goulding, and M. C. Field.** 2003. Clathrin-mediated endocytosis is essential in *Trypanosoma brucei.* EMBO J. **22:**4991–5002.
2. **Bangs, J. D., L. Uyetake, M. J. Brickman, A. E. Balber, and J. C. Boothroyd.** 1995. Molecular cloning and cellular localization of a BiP homologue in *Trypanosoma brucei.* Divergent ER retention signals in a lower eukaryote. J. Cell Sci. **105:**1101–1113.
3. **Brickman, M. J., J. M. Cook, and A. E. Balber.** 1995. Low temperature reversibly inhibits transport from tubular endosomes to a perinuclear, acidic compartment in African trypanosomes. J. Cell Sci. **108:**3611–3621.
4. **Chen, W., Y. Feng, D. Chen, and A. Wandinger-Ness.** 1998. Rab11 is required for *trans*-Golgi network-to-plasma membrane transport and a preferential target for GDP dissociation inhibitor. Mol. Biol. Cell **9:**3241–3257.
5. **Cheng, H., R. Sugiura, W. Wu, M. Fujita, Y. Lu, S. O. Sio, R. Kawai, K. Takegawa, H. Shuntoh, and T. Kuno.** 2002. Role of the Rab GTP-binding protein Ypt3 in the fission yeast exocytic pathway and its connection to calcineurin function. Mol. Biol. Cell **13:**2963–2976.
6. **de Graaf, P., W. T. Zwart, R. A. van Dijken, M. Deneka, T. K. Schulz, N. Geijsen, P. J. Coffer, B. M. Gadella, A. J. Verkleij, P. van der Sluijs, and P. M. van Bergen en Henegouwen.** 2004. Phosphatidylinositol 4-kinaseβ is critical for functional association of rab11 with the Golgi complex. Mol. Biol. Cell **15:**2038–2047.
7. **Dhir, V., D. Goulding, and M. C. Field.** 2004. TbRAB1 and TbRAB2 mediate trafficking through the early secretory pathway of *Trypanosoma brucei.* Mol. Biochem. Parasitol. **137:**253–265.
8. **Engstler, M., L. Thilo, F. Weise, C. Grunfelder, H. Schwarz, and M. Boshart.** 2004. Kinetics of endocytosis and recycling of the GPI-anchored variant surface glycoprotein of *Trypanosoma brucei.* J. Cell Sci. **17:**1105–1115.
9. **Fan, G. H., L. A. Lapierre, J. R. Goldenring, and A. Richmond.** 2003. Differential regulation of CXCR2 trafficking by Rab GTPases. Blood **101:**2115–2124.
10. **Fast, B., K. Kremp, M. Boshart, and D. Steverding.** 1999. Iron-dependent regulation of transferrin receptor expression in *Trypanosoma brucei.* Biochem. J. **342:**691–696.
11. **Field, H., M. Farjah, A. Pal, K. Gull, and M. C. Field.** 1998. Complexity of trypanosomatid endocytosis pathways revealed by Rab4 and Rab5 isoforms in *Trypanosoma brucei.* J. Biol. Chem. **273:**32102–32110.
12. **Grunfelder, C. G., M. Engstler, F. Weise, H. Schwarz, Y. D. Stierhof, G. M. Morgan, M. C. Field, and P. Overath.** 2003. Endocytosis of a GPI-anchored protein via clathrin-coated vesicles, sorting by default in endosomes and exocytosis via Rab11-positive carriers. Mol. Biol. Cell **14:**2029–2040.
13. **Hales, C. M., R. Griner, K. C. Hobdy-Henderson, M. C. Dorn, D. Hardy, R. Kumar, J. Navarre, E. K. Chan, L. A. Lapierre, and J. R. Goldenring.** 2001. Identification and characterization of a family of Rab11-interacting proteins. J. Biol. Chem. **276:**39067–39075.
14. **Hall, B. S., A. Pal, D. Goulding, and M. C. Field.** 2004. Rab4 is an essential regulator of lysosomal trafficking in trypanosomes. J. Biol. Chem. **279:**45047–45056.
15. **Hall, B. S., C. L. Allen, D. Goulding, and M. C. Field.** 2004. The small GTPases TbRAB5A and TbRAB5B are both essential and required for endocytosis in bloodstream form *T. brucei.* Mol. Biochem. Parasitol. **138:**67–77.
16. **Hunyady, L., A. J. Baukal, Z. Gaborik, J. A. Olivares-Reyes, M. Bor, M. Szaszak, R. Lodge, K. J. Catt, and T. Balla.** 2002. Differential PI 3-kinase dependence of early and late phases of recycling of the internalized AT1 angiotensin receptor. J. Cell Biol. **157:**1211–1222.
17. **Jeffries, T. R., G. W. Morgan, and M. C. Field.** 2001. A developmentally regulated rab11 homologue in *Trypanosoma brucei* is involved in recycling processes. J. Cell Sci. **114:**2617–2626.
18. **Kelley, R. J., M. J. Brickman, and A. E. Balber.** 1995. Processing and transport of a lysosomal membrane glycoprotein is developmentally regulated in African trypanosomes. Mol. Biochem. Parasitol. **74:**167–178.
19. **Khvotchev, M. V., M. Ren, S. Takamori, R. Jahn, and T. C. Sudhof.** 2003. Divergent functions of neuronal Rab11b in Ca^{2+}-regulated versus constitutive exocytosis J. Neurosci. **23:**10531–10539.
20. **Kreuzer, O. J., B. Krisch, O. Dery, N. W. Bunnett, and W. Meyerhof.** 2001. Agonist-mediated endocytosis of rat somatostatin receptor subtype 3 involves β-arrestin and clathrin coated vesicles. J. Neuroendocrinol. **13:**279–287.
21. **LaCount, D. J., S. Bruse, K. L. Hill, and J. E. Donelson.** 2000. Double-stranded RNA interference in *Trypanosoma brucei* using head-to-head promoters. Mol. Biochem. Parasitol. **111:**67–76.
22. **Lapierre, L. A., R. Kumar, C. M. Hales, J. Navarre, S. G. Bhartur, J. O. Burnette, D. W. Provance, Jr., J. A. Mercer, M. Bahler, and J. R. Goldenring.**

2001. Myosin Vb is associated with plasma membrane recycling systems. Mol. Biol. Cell **12:**1843–1857.

23. **Liu, J., X. Qiao, D. Du, and M. G.-S. Lee.** 2000. Receptor-mediated endocytosis in the procyclic form of *Trypanosoma brucei*. J. Biol. Chem. **16:**12032–12040.

24. **Mammoto, A., T. Ohtsuka, I. Hotta, T. Sasaki, and Y. Takai.** 1999. Rab11BP/Rabphilin-11, a downstream target of rab11 small G protein implicated in vesicle recycling. J. Biol. Chem. **274:**25517–25524.

25. **McGugan, G. C., Jr., and L. A. Temesvari.** 2003. Characterization of a Rab11-like GTPase, EhRab11, of *Entamoeba histolytica*. Mol. Biochem. Parasitol. **129:**137–146.

26. **Mitchell, H., A. Choudhury, R. E. Pagano, and E. B. Leof.** 2004. Ligand-dependent and -independent transforming growth factor-β receptor recycling regulated by clathrin-mediated endocytosis and Rab11. Mol. Biol. Cell **15:**4166–4178.

27. **Moore, R. H., E. E. Millman, E. Alpizar-Foster, W. Dai, B. J. Knoll.** 2004. Rab11 regulates the recycling and lysosome targeting of β2-adrenergic receptors. J. Cell Sci. **117:**3107–3117.

28. **Morgan, G. W., C. L. Allen, T. R. Jeffries, M. Hollinshead, and M. C. Field.** 2001. Developmental and morphological regulation of clathrin-mediated endocytosis in *Trypanosoma brucei*. J. Cell Sci. **114:**2605–2615.

29. **Morgan, G. W., B. S. Hall, P. W. Denny, M. Carrington, and M. C. Field.** 2002. The kinetoplastida endocytic apparatus. Part I: a dynamic system for nutrition and evasion of host defences. Trends Parasitol. **18:**491–496.

30. **Mussmann, R., H. Janssen, J. Calafat, M. Engstler, I. Ansorge, C. Clayton, and P. Borst.** 2003. The expression level determines the surface distribution of the transferrin receptor in *Trypanosoma brucei*. Mol. Microbiol. **47:**23–35.

31. **Overath, P., and M. Engstler.** 2004. Endocytosis, membrane recycling and sorting of GPI-anchored proteins: *Trypanosoma brucei* as a model system. Mol. Microbiol. **53:**735–744.

32. **Pal, A., B. S. Hall, D. N. Nesbeth, H. L. Field, and M. C. Field.** 2002. Differential endocytic functions of *Trypanosoma brucei* Rab5 isoforms reveal a glycosylphosphatidylinositol-specific endosomal pathway. J. Biol. Chem. **277:**9529–9539.

33. **Pal, A., B. S. Hall, T. Jefferies, and M. C. Field.** 2003. Rab5 and Rab11 mediate transferrin and anti-variant surface glycoprotein antibody recycling in *Trypanosoma brucei*. Biochem. J. **374:**443–451.

34. **Riggs, B., W. Rothwell, S. Miscue, G. R. Hickson, J. Matheson, T. S. Hays, G. W. Gould, and W. Sullivan.** 2003. Actin cytoskeleton remodelling during early *Drosophila* furrow formation requires recycling endosomal components Nuclear-fallout and Rab11. J. Cell Biol. **163:**143–154.

35. **Sharma, D. K., A. Choudhury, R. D. Singh, C. L. Wheatley, D. L. Marks, and R. E. Pagano.** 2003. Glycosphingolipids internalized via caveolar-related endocytosis rapidly merge with the clathrin pathway in early endosomes and form microdomains for recycling. J. Biol. Chem. **278:**7564–7572.

36. **Ullrich, O., S. Reinsch, S. Urbe, M. Zerial, and R. G. Parton.** 1996. Rab11 regulates recycling through the pericentriolar recycling endosome. J. Cell Biol. **135:**913–924.

37. **Volpicelli, L. A., J. J. Lah, G. Fang, J. R. Goldenring, and A. I. Levey.** 2002. Rab11a and myosin Vb regulate recycling of the M4 muscarinic acetylcholine receptor. J. Neurosci. **22:**9776–9784.

38. **Wallace, D. M., A. J. Lindsay, A. G. Hendrick, and M. W. McCaffrey.** 2002. The novel Rab11-FIP/Rip/RCP family of proteins displays extensive homo- and hetero-interacting abilities. Biochem. Biophys. Res. Commun. **292:**909–915.

39. **Wang, X., R. Kumar, J. Navarre, J. E. Casanova, and J. R. Goldenring.** 2000. Regulation of vesicle trafficking in madin-darby canine kidney cells by Rab11a and Rab25. J. Biol. Chem. **275:**29138–29146.

40. **Wilcke, M., L. Johannes, T. Galli, V. Mayau, B. Goud, and J. Salamero.** 2000. Rab11 regulates the compartmentalization of early endosomes required for efficient transport from early endosomes to the *trans*-Golgi network. J. Cell Biol. **151:**1207–1220.

41. **Wirtz, E., S. Leal, C. Ochatt, and G. A. Cross.** 1999. A tightly regulated inducible expression system for conditional gene knock-outs and dominant-negative genetics in *Trypanosoma brucei*. Mol. Biochem. Parasitol. **99:**89–101.

42. **Zerial, M., and H. McBride.** 2001. Rab proteins as membrane organizers. Nat. Rev. Mol. Cell Biol. **2:**107–117.

43. **Zhang, X. M., S. Ellis, A. Sriratana, C. A. Mitchell, and T. Rowe.** 2004. Sec15 is an effector for the Rab11 GTPase in mammalian cells. J. Biol. Chem. **279:**43027–43034.